Journal of Nuclear Materials 495 (2017) 516–528

Contents lists available at ScienceDirect

Journal of Nuclear Materials

journal homepage: www.elsevier.com/locate/jnucmat

Microstructure evolution of recrystallized Zircaloy-4 under charged particles irradiation

M. Gaumé [a, *], F. Onimus [a], L. Dupuy [a], O. Tissot [a], C. Bachelet [b], F. Mompiou [c]

[a] DEN, Service de Recherches de Métallurgie Appliquées, CEA Saclay, Université Paris-Saclay, F-91191 Gif-sur-Yvette, France
[b] CSNSM, Université Paris-Sud, CNRS/IN2P3, Université Paris-Saclay, 91405 Orsay, France
[c] CEMES CNRS, 29 Rue Jeanne Marvig, 31055 Toulouse Cedex 4, France

GRAPHICAL ABSTRACT

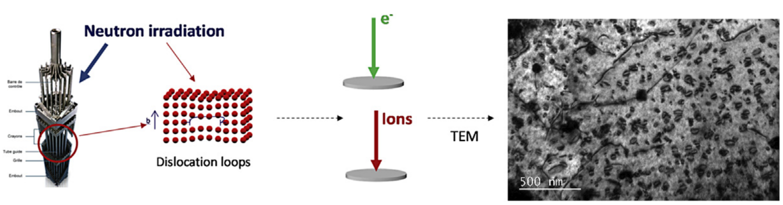

ARTICLE INFO

Article history:
Received 5 May 2017
Received in revised form
28 July 2017
Accepted 4 September 2017
Available online 8 September 2017

Keywords:
Recrystallized Zircaloy-4
Electron irradiation
Ion irradiation
<a> loops
High voltage electron microscope
Transmission electron microscopy

ABSTRACT

Recrystallized zirconium alloys are used as nuclear fuel cladding tubes of Pressurized Water Reactors. During operation, these alloys are submitted to fast neutron irradiation which leads to their in-reactor deformation and to a change of their mechanical properties. These phenomena are directly related to the microstructure evolution under irradiation and especially to the formation of <a>-type dislocation loops. In the present work, the radiation damage evolution in recrystallized Zircaloy-4 has been studied using charged particles irradiation. The <a> loop nucleation and growth kinetics, and also the helical climb of <a> linear dislocations, were observed *in-situ* using a High Voltage Electron Microscope (HVEM) under 1 MeV electron irradiation at 673 and 723 K. In addition, 600 keV Zr^+ ion irradiations were conducted at the same temperature. Transmission Electron Microscopy (TEM) characterizations have been performed after both types of irradiations, and show dislocation loops with a <a> Burgers vector belonging to planes close to $\{10\bar{1}0\}$ first order prismatic planes. The nature of the loops has been characterized. Only interstitial <a> dislocation loops have been observed after ion irradiation at 723 K. However, after electron irradiation conducted at 673 and 723 K, both interstitial and vacancy loops were observed, the proportion of interstitial loops increasing as the temperature is increased. The loop growth kinetics analysis shows that as the temperature increases, the loop number density decreases and the loop growth rate tends to increase. An increase of the flux leads to an increase of the loop number density and a decrease of the loop growth rate. The results are compared to previous works and discussed in the light of point defects diffusion.

1. Introduction

Zirconium alloys are used as nuclear fuel cladding tube material of Pressurized Water Reactors (PWR). In-reactor, the material is submitted to fast neutron irradiation which modifies its mechanical

* Corresponding author.
E-mail addresses: marine.gaume@cea.fr (M. Gaumé), fabien.onimus@cea.fr (F. Onimus).

http://dx.doi.org/10.1016/j.jnucmat.2017.09.004
0022-3115/

properties leading to its strengthening and to a loss of macroscopic ductility. Furthermore, during operation, the cladding exhibits a macroscopic deformation, mainly due to irradiation creep and growth. These different phenomena find their origin in the microstructure evolution under irradiation [1]. In order to have a better understanding and a physically based prediction of the cladding tubes behavior under irradiation, a thorough characterization of the microstructure is required.

The microstructure evolution of zirconium alloys under neutron irradiation has been well characterized, especially during the 70's, [2–6] and later reviewed by Griffiths [7]. The damage structure consists mainly of <a>-type dislocation loops located close to the prismatic planes of the Hexagonal Close Packed structure with $\frac{1}{3}<11\bar{2}0>$ type Burgers vectors. These loops were found to be non-edge in character, the loop normal being tilted towards the $<1\bar{1}00>$ direction with an additional slight tilt towards the <0001> direction. The loops are nearly circular, the ellipticity (the ratio b/a between the short axis b and the major axis a), being between 0.8 and 1 for loop diameter below 50 nm [3]. They appear at the beginning of the irradiation, and the loop size and density tend to saturate as the dose increases [8]. Surprisingly, both vacancy and interstitial loops coexist [3], while it is expected that only interstitial dislocation loops can grow.

The change of mechanical properties under irradiation has been clearly correlated to the evolution of <a> loops. Despite the early extensive studies, the detailed mechanisms at the origin of the <a> loop evolution are still not clearly understood. For instance, there is still no clear explanation for the coexistence of both vacancy and interstitial <a>-loops. Furthermore, the dislocation climb under irradiation, which may play a role in the irradiation creep phenomenon, has not been studied. Moreover, the potential anisotropic diffusion of self-interstitial atoms under irradiation, which is believed to be at the origin of the irradiation induced growth, remains a matter of debate. In order to gain a better understanding of radiation damage evolution and, in a future prospect, to develop a predictive physically based model to simulate this evolution, accurate and parametric experiments are still needed.

Because neutron irradiation experiments are long, expensive and lead to difficult handling of the radioactive samples, charged particle irradiations are often used in the nuclear materials field to emulate neutron irradiation [9]. High doses can be achieved in a relatively short time (from few hours to several days) by charged particles irradiation. They do not activate the material and the microstructure characterization can be performed *in-situ* in a TEM, in some facilities.

In the past, the <a>-loop evolution has been studied at different temperatures, mainly using in situ High Voltage Electron Microscope (HVEM) irradiations [10–17]. Detailed analysis of the kinetics of <a>-loop evolution at different temperatures has been done by Hellio et al. [16] and Nakamichi et al. [17]. Hellio et al. [16] have also studied the effect of the alloying elements on the dislocation loops kinetics and have shown that in a Zr-0 alloy, the loop density is higher and the loop size is smaller than in pure Zr. Several authors also conducted a detailed analysis of the loop habit plane and loop nature. Carpenter and Watters [11] showed that <a>-loops were all interstitial in nature in pure zirconium at 725 K. On the other hand, for temperatures ranging from 675 K up to 730 K, Griffiths et al. [14] observed both vacancy and interstitial <a>-loops in pure zirconium. Concerning Zircaloys, Nakamichi et al. [17] found that at high temperature of 770 K, the loops were all of interstitial type. The same result has been observed by Hellio et al. [16] after 1 MeV electron irradiation at temperatures higher than 773 K on a Zr-1760 ppm O. However, and contrary to the results obtained by Griffiths [14] in pure zirconium, the coexistence of interstitial and vacancy loops under electron irradiation has never been observed for zirconium alloys.

Furthermore, only very few authors have used heavy ions to study the <a>-loop evolution under irradiation. Early works are reported by Lee and Koch [18] and Adamson et al. [19], using 5 MeV Ni ion irradiation. Hellio et al. [16] also conducted 500 keV Zr ion irradiation of pure zirconium and various zirconium alloys at temperatures ranging from 673 K to 723 K. Some information concerning the effect of temperature and alloying elements on loop size and density are given by these authors. Recently several studies used in situ 1 MeV Kr ion irradiation from 573 K up to 773 K [20,21]. In these experiments the <a>-loops were always very small and numerous and no loop nature analysis was attempted.

The evolution under irradiation of linear dislocations with <a> Burgers vector has not been studied in details by any authors. Buckley and Manthorpe [10] show a picture of helical climb of <a>-dislocation at 773 K under electron irradiation. A similar observation has been done by Griffiths et al. [12]. Nothing is known concerning the climb kinetics of <a>-dislocations under irradiation.

In order to have a better understanding of the <a>-loop formation and <a>-dislocation climb under irradiation a new study has been undertaken using both, in situ 1 MeV electron irradiation and 600 keV Zr ion irradiation, at temperatures ranging from 673 K to 723 K. This study focusses mainly on the loop growth kinetics under irradiation and on the loop nature after irradiation. The helical climb of <a>-dislocation under irradiation is also studied. The results are discussed in comparison with previous works and in the light of point defects diffusion mechanisms.

2. Experimental techniques

2.1. Studied material

Recrystallized Zircaloy-4, often considered as a model material for recrystallized zirconium alloys, has been studied. The as-received recrystallized Zircaloy-4, referred to as RXA Zircaloy-4 (RXA meaning recrystallization annealing), exhibits a homogeneous microstructure made of equi-axed grains with an average diameter of 6.2 ± 0.6 μm. The samples have been taken out of a rolled thin sheet of 0.42 mm thick. This rolled sheet exhibits a crystallographic texture with the c-axis of the grains tilted at an angle of about 25°–30° to the Normal Direction (ND) of the rolled sheet, in the ND-TD plane (TD referring to the Transverse Direction).

Thanks to the relatively large grains containing only few dislocations (typically 10^{11} m^{-2} when measured by using the line intercept method [22]), the radiation damage evolution, and especially the <a>-type loops, can be well analyzed in this material using Transmission Electron Microscopy (TEM). However, in order to analyze more easily the dislocation climb mechanism under irradiation, the rolled sheet has been strained up to 1% plastic strain at room temperature prior to irradiation. During the plastic deformation, <a>-dislocations have been created, leading to a microstructure containing a significant amount of dislocations (typically 10^{13} m^{-2}).

Samples have been taken out of the rolled sheet in the TD-RD plane (RD referring to the Rolling Direction). The samples were first mechanically polished and 3 mm diameter disks were punched out. The samples used for in situ electron irradiation were double-side jet electropolished using an electrolytic solution of 90% ethanol and 10% perchloric acid at 263 K. The samples used for Zr ion irradiation were first jet electropolished on one side only. After irradiation, the irradiated surface was then protected by a lacquer and the samples were electropolished on the back side up to create a hole surrounded by thin area, required for TEM observations.

2.2. Charged particles irradiation

2.2.1. Electron irradiation

In-situ electron irradiations were performed in a Kratos HVEM at CEA-Saclay, operated at 1 MV, using a single tilt heating sample holder. Experiments were performed at two temperatures of 673 K and 723 K. These temperatures were measured thanks to a thermocouple attached to the specimen holder. During the experiment, the electron current was measured and the damage rate was calculated using a displacement cross section of 35 b, related to a displacement energy of 25 eV [23]. Indeed, Griffiths [24] reported that the displacement energy ranges from 24 eV to 27.5 eV depending on the crystallographic orientation considered. The calculated flux ranged from 3.6×10^{21} and 6×10^{21} $e^-.m^{-2}.s^{-1}$ for the lower flux and is equal to 3.6×10^{22} $e^-.m^{-2}.s^{-1}$ for the higher flux. This gives a damage rate respectively of about $1{-}2 \times 10^{-5}$ dpa. s^{-1} and 1×10^{-4} dpa. s^{-1}. The irradiation time, ranging from 20 min up to 1 h, leads to doses up to 0.064 dpa for the lower flux and up to 0.37 dpa for the higher flux. During the experiments, the electron beam was spread, allowing the use of a CCD camera to record *in-situ* the microstructure evolution under irradiation by taking a picture every 30 s. An additional electron irradiation has been conducted at a higher temperature of 853 K, and for a higher flux of 8.4×10^{23} $e^-.m^{-2}.s^{-1}$. However, due to the highly focused beam, the observation was not performed *in-situ*. Only a post-irradiation analysis was therefore performed on this sample.

2.2.2. Ion irradiations

600 keV Zr^+ ion irradiations have been conducted on the ARAMIS-facility at CSNSM/IN2P3 Orsay. Two irradiation temperatures of 673 and 723 K were applied and the specimens were irradiated up to two fluences: 8×10^{17} ions. m^{-2} and 24×10^{17} ions. m^{-2}. The damage profile obtained is illustrated on Fig. 1 for a dose of 8×10^{17} ions. m^{-2}. This profile has been obtained thanks to the SRIM software, using the "Quick calculation of damage" mode [25]. A displacement threshold energy of 25 eV has been used, in order to be consistent with the electron damage calculation, although according to standards [25], a displacement energy of 40 eV is often considered for zirconium. It can be seen that the thin foil thickness (of 150 nm thick) is fully irradiated. The average damage dose over the foil thickness has been calculated and gives damage doses respectively of 0.45 dpa for a fluence of 8×10^{17} ions. m^{-2} and 1.36 dpa for a fluence of 24×10^{17} ions. m^{-2}. The damage rate was about 10^{-4} dpa. s^{-1}. It can be seen on Fig. 1 that the implanted Zr ions peak is around 200 nm deep below the surface. By using self-ions, a limited effect of ion implantation is expected.

The irradiation conditions under 1 MeV electron and 600 keV Zr^+ ion irradiations are summarized in Table 1.

2.3. TEM analysis

The TEM analyses have been performed on a JEOL 2100 microscope operating at 200 kV using a double-tilt sample holder. As described previously, the c-axis of most of the grains is tilted about 25°–30° from the Normal Direction (ND) of the foil. By aligning the Rolling Direction (RD) parallel to the primary tilt axis, it is therefore possible to easily reach a $<11\overline{2}3>$ zone axis by tilting less than 20°. Indeed, <a>-loops can be well observed with a beam close to the $<11\overline{2}3>$ direction and using either $\mathbf{g} = 11\overline{2}2$ or $\mathbf{g} = 10\overline{1}1$ types diffraction vectors.

3. Results

3.1. Nucleation and growth kinetics of dislocation loops

3.1.1. In-situ electron irradiations

During *in-situ* experiments under 1 MeV electron irradiation, the nucleation and growth of <a>- loops have been observed. As seen on Fig. 2 (723 K), the loops can be seen from very low doses, of the order of 0.015 dpa, in the form of black dots. They progressively grow, appearing elliptical with the typical "coffee-bean" contrast. For bigger loops, a nice elliptical shape line can be seen.

Fig. 3 presents the evolution of the number density and the mean diameter of <a>-loops as a function of irradiation damage for two grains irradiated at 673 K (410 loops analyzed) and one grain irradiated at 723 K (96 loops analyzed) and for flux ranging from 3.6×10^{21} to 6×10^{21} $e^-.m^{-2}.s^{-1}$. For some grains, when possible, the foil thickness has been measured using Electron Energy Loss Spectroscopy (EELS) (accuracy of ±15%). If the EELS measurement was not performed, the foil thickness was considered to be equal to 200 nm ± 30%. It can be seen that both, the loop number density and the loop diameter, increase with dose. No clear saturation of the loop density is observed for these low doses. It can be noticed that an increase of the irradiation temperature leads to a decrease of the number density and a slight increase of the loop mean diameter for a given dose rate, in agreement with previous results [16,17].

The effect of flux has also been studied for an irradiation temperature of 723 K. Fig. 4 presents the evolution of the loop number density and mean diameter for two fluxes studied, up to a similar dose of 0.15 dpa: 6×10^{21} $e^-.m^{-2}.s^{-1}$ and 3.6×10^{22} $e^-.m^{-2}.s^{-1}$. This result demonstrates an effect of the applied flux on the loop evolution at 723 K. Indeed, an increase of the flux leads to an increase of the number density and a decrease of the mean loop diameter.

3.1.2. Ion irradiations

As for electron irradiations, ion irradiations are often used to emulate neutron irradiation. Three irradiations have been performed using 600 keV Zr ions at 673 K and 723 K up to 0.45 dpa and at 723 K up to 1.36 dpa. The three typical microstructures resulting from these irradiations are presented on Fig. 5. When increasing the irradiation temperature, a decrease of the loop number density is observed, from 3.2×10^{21} m^{-3} at 673 K down to 6.4×10^{20} m^{-3} at 723 K. Moreover, a significant increase in the mean loop diameter is also observed, increasing from 13 nm at 673 K up to 32 nm at 723 K. On the other hand, when the damage dose is increased from 0.45 dpa to 1.36 dpa, no clear effect on the final microstructure is observed. Indeed, the loop number densities are equal to 6.4×10^{20} m^{-3} and 5.6×10^{20} m^{-3} respectively for doses of 0.45 dpa to 1.36 dpa, and the mean loop diameter are respectively 32 nm and 35 nm. The loop size distributions for the three irradiations are shown on Fig. 6. A large number of loops have been analyzed: 1553 loops in three grains at 673 K and 0.45 dpa, 1863 loops in two grains at 723 K and 0.45 dpa and 2384 loops in four grains at 723 K and 1.36 dpa. It can be noticed that for the irradiation conducted at 723 K, some loops with very large diameter, typically above 110 nm, can be observed.

The foil thickness was measured for several grains using EELS method. This measurement shows that the mean thickness of the studied grains is close to 150 nm.

3.2. Dislocation loop characterization

3.2.1. Loop Burgers vector determination

The loop Burgers vector has been determined using the

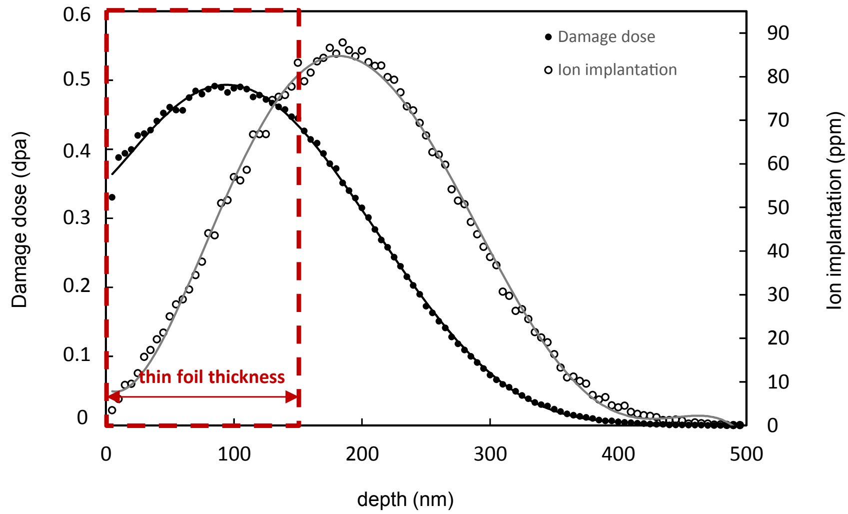

Fig. 1. SRIM calculations of the damage and ion implantation profiles for 600 keV Zr + ions and for a fluence of 8.10^{17} ions. m^{-2}.

Table 1
Electron and ion irradiation conditions.

Irradiation type	Temperature (K)	Flux (particles.m^{-2}.s^{-1})	Damage rate (dpa.s^{-1})	Final dose (dpa)
1 MeV e^-	673	3.6×10^{21}	1×10^{-5}	0.03
1 MeV e^-	673	3.6×10^{21}	1×10^{-5}	0.04
1 MeV e^-	723	6×10^{21}	2×10^{-5}	0.064
1 MeV e^-	723	3.6×10^{22}	1×10^{-4}	0.37
1 MeV e^-	853	8.4×10^{23}	3×10^{-3}	3.6
600 keV Zr^+	673	2.2×10^{14}	1×10^{-4}	0.45
600 keV Zr^+	723	2.2×10^{14}	1×10^{-4}	0.45
600 keV Zr^+	723	2.2×10^{14}	1×10^{-4}	1.36

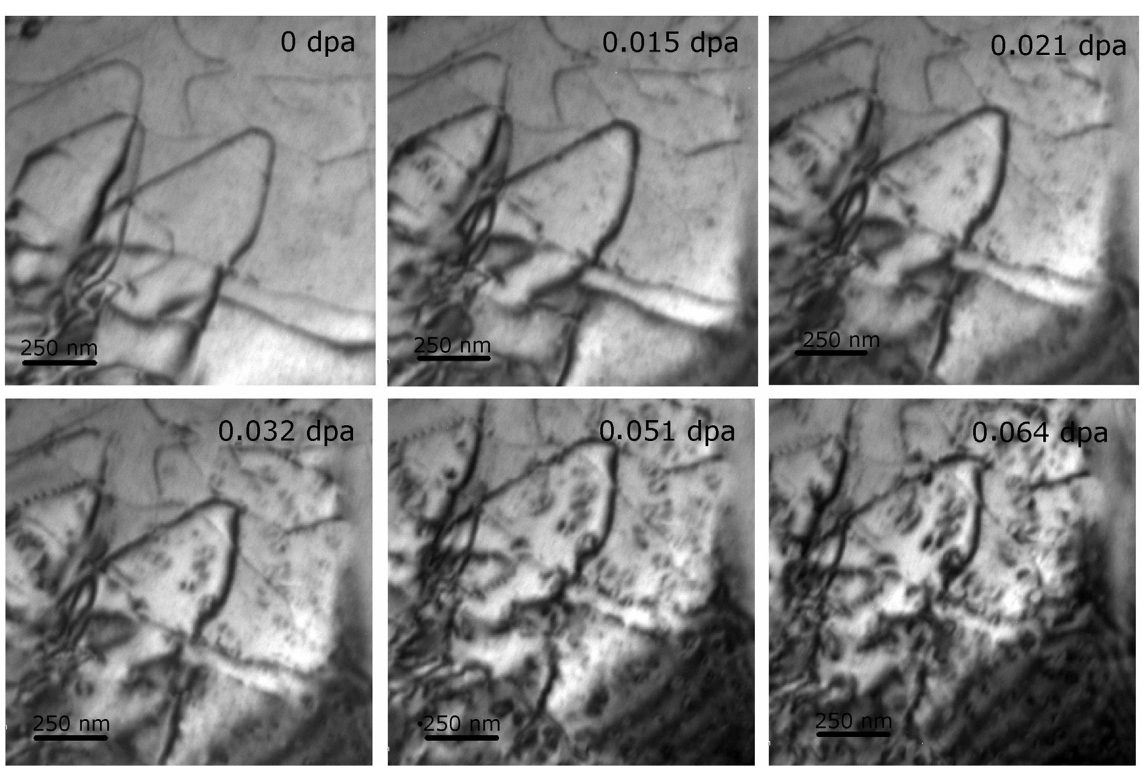

Fig. 2. Microstructure evolution under 1 MeV electron irradiation at 723 K on pre-strained RXA Zircaloy-4.

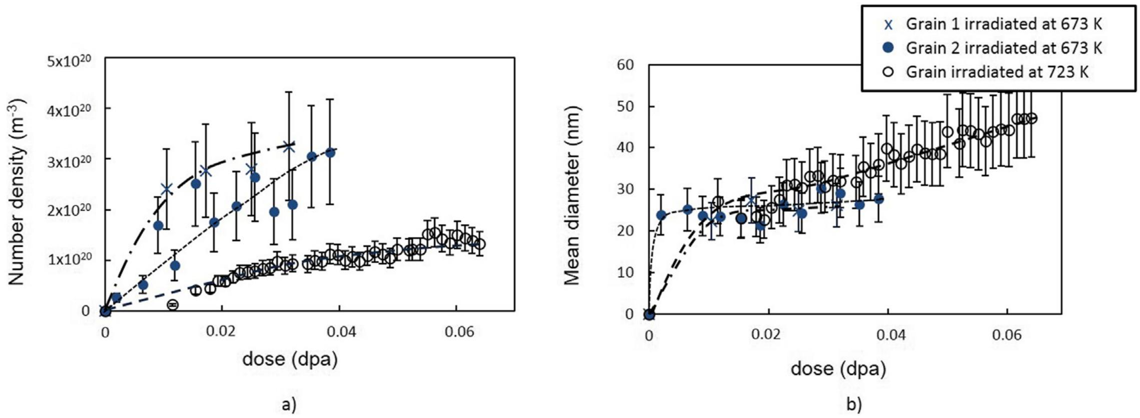

Fig. 3. Evolution of the a) number density and b) the mean diameter of the dislocation loops as a function of the dose under 1 MeV electron irradiation at 673 K and 723 K, electron flux ranged from 3.6×10^{21} and 6×10^{21} $e^{-}.m^{-2}.\ s^{-1}$.

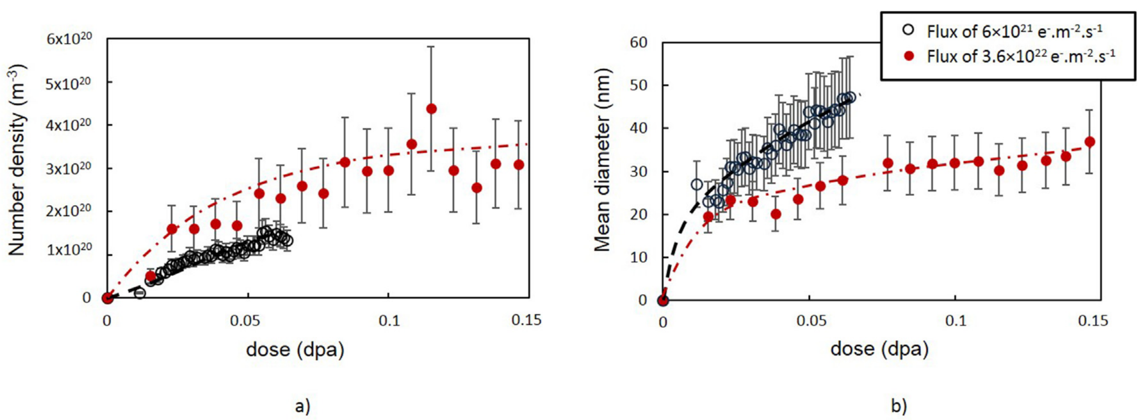

Fig. 4. Evolution of the a) number density and b) the mean diameter of the dislocation loops as a function of the dose under 1 MeV electron irradiation at 723 K for two fluxes: 6.10^{21} and 3.6×10^{22} $e^{-}.m^{-2}.\ s^{-1}$.

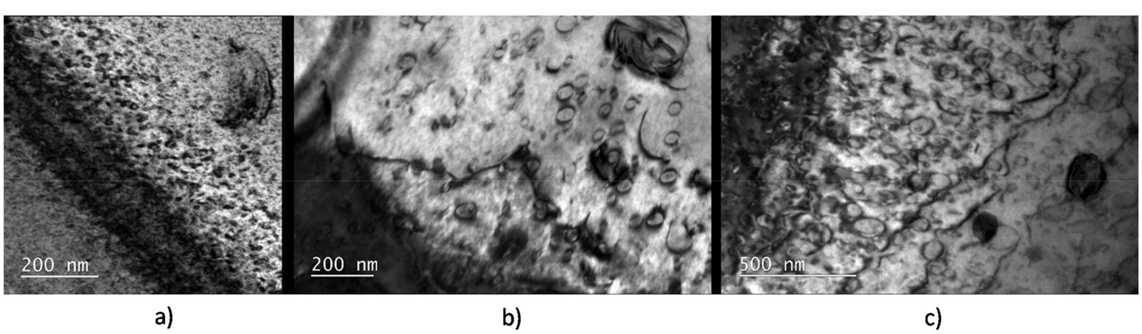

Fig. 5. Zr^{+} 600 keV irradiation microstructures of RXA Zircaloy-4 at a) 673 K and 0.45 dpa b) 723 K and 0.45 dpa c) 723 K and 1.36 dpa.

invisibility criterion $\mathbf{g.b} = 0$, $\mathbf{g}$ being the diffraction vector in two beam condition. The loops were assumed to be only <a> type loops. Indeed, according to Griffiths [13], the total loop population is composed of around 90% of <a> type loops. However, some of the loops may also have a <c+a> Burgers vectors of $\frac{1}{3}<1\bar{2}13>$ type, as reported by Griffiths et al. [12,13]. To insure that these loops are not <c+a> loops, the use of the diffraction vector g = 0002 would have been required. However, due to the orientation of the studied grain, this analysis was not possible. Fig. 7 gives an example of this TEM analysis after 600 keV Zr irradiation at 723 K and for dose of 0.45 dpa. The same analysis has been performed for the other ion irradiation conditions and for the electron irradiations and proves that loops with the three <a> Burgers vectors coexist. In this example, four diffraction vectors were chosen. The loop contrast noted A and B are clearly visible for $\mathbf{g_1} = 1\bar{2}12$, $\mathbf{g_2} = 1\bar{1}01$ and $\mathbf{g_3}$ $=0\bar{1}11$ but are invisible for $\mathbf{g_4} = 10\bar{1}0$. Similarly, loops C and D are clearly visible for $\mathbf{g_1}$, $\mathbf{g_2}$ and $\mathbf{g_4}$ but are invisible for $\mathbf{g_3}$. It can be therefore deduced that the Burgers vectors of loops A and B are $\frac{1}{3}[1\bar{2}10]$ and the Burgers vectors of loops C and D is $\frac{1}{3}[\bar{2}110]$. On Fig. 7, the stereographic projection gives the orientation of the grain. The angle λ between the foil normal N and the <c> axis has

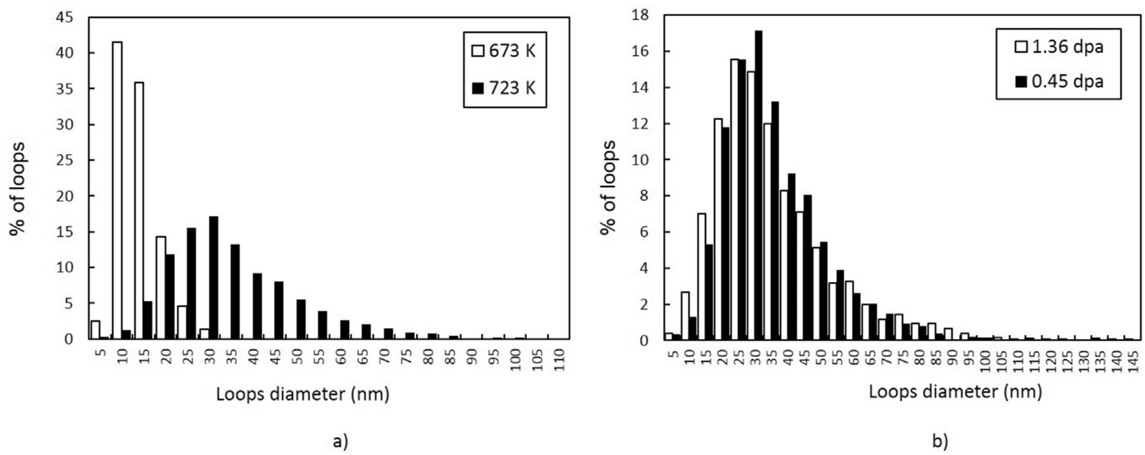

Fig. 6. Distribution of the loop diameter after Zr+ 600 keV ion irradiation a) effect of the temperature for a dose of 0.45 dpa and b) effect of the dose at 723 K.

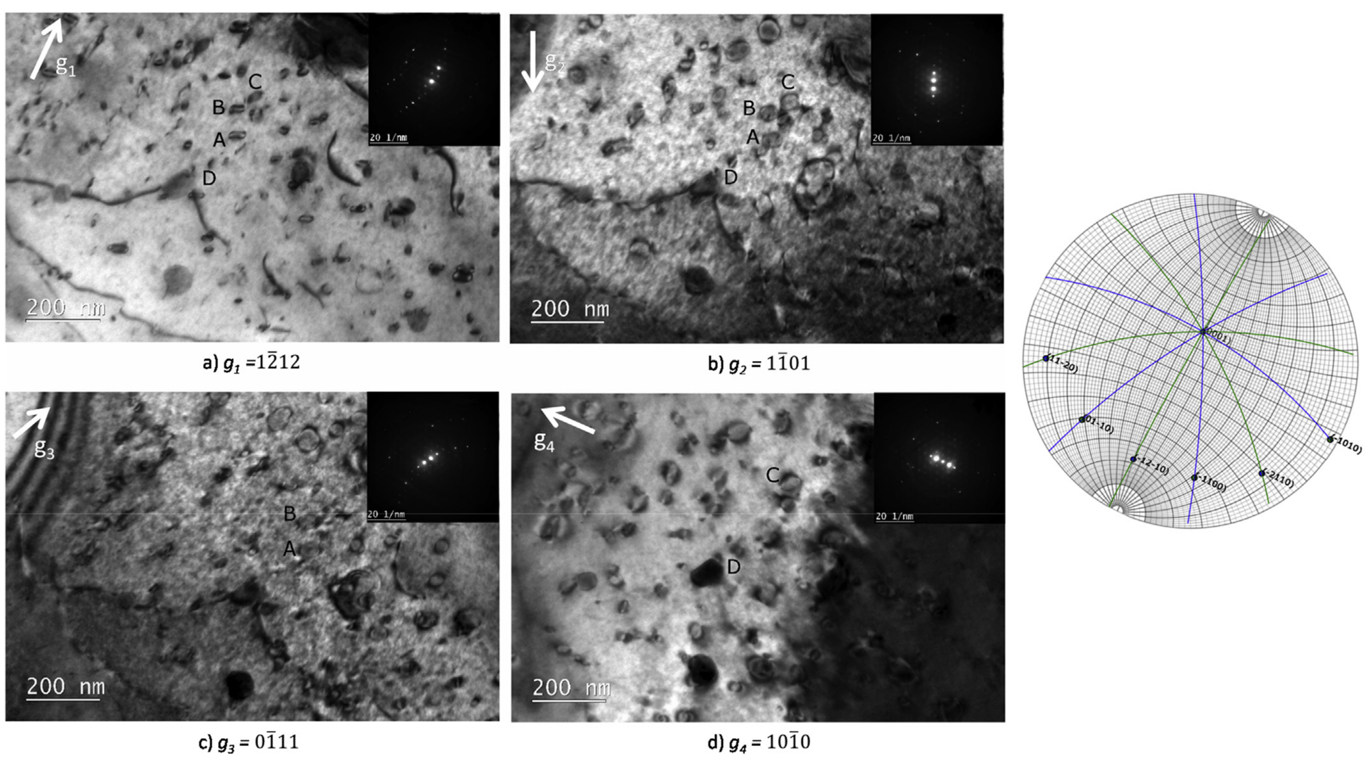

Fig. 7. Loop Burgers vectors determination using the extinction method on a 600 keV Zr^+ ion irradiated RXA Zircaloy-4 at 623 K up to 0.45 dpa. Angle between the foil normal N and <c>: λ = 26°. The stereographic projection is given for a 0° tilt angle.

also been systematically measured. The stereographic projection of the grain is also given on Fig. 7 and the traces of the first order prismatic planes {10$\bar{1}$0} are given in green, and the traces of the second order prismatic planes {11$\bar{2}$0} are given in blue.

3.2.2. Habit plane determination

Following the work done by Carpenter and Watters [11], an approximate loop habit plane analysis has been carried out. In this method, it is assumed that the loops are nearly circular. Indeed, in the literature [6] it is shown that for loops with diameter lower than 50 nm the ellipticity ratio (b/a) lies between 0.8 and 1. The loops are tilted with respect to the beam direction and thus appear as ellipses with a long axis direction perpendicular to the habit plane normal. Thus, if the normal of the habit plane is assumed to be in the (0001) plane, the direction of the long axis of the loop allows the measurement of the rotation angle θ about the c-axis relative to the pure edge orientation. Indeed if the <a> loops were pure edge loops, their habit plane would have been the {11$\bar{2}$0} planes. This analysis has been performed for both 1 MeV electron and 600 keV Zr ion irradiated samples. As an example, the plane normal directions of <a> loops, observed in one grain after ion irradiation, are indicated in the standard stereographic triangle in Fig. 8 as inverse pole figure. It is shown that the majority of loops tends to be tilted away from the {$\bar{1}$2$\bar{1}$0} plane at angles up to 30°, and are therefore closer to the first order prismatic plane {$\bar{1}$100}. This analysis has shown that the loops do not strictly belong to the

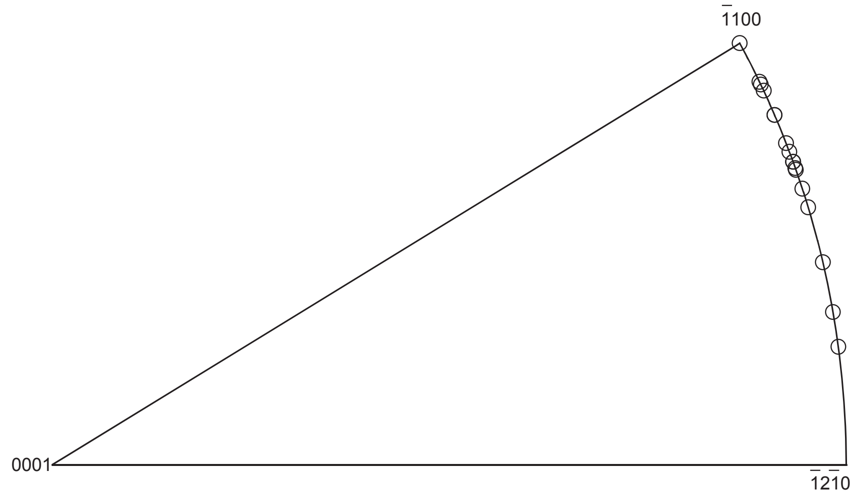

Fig. 8. Distribution of the loop plane normal for loops with a Burgers vector $\frac{1}{3}<\bar{1}2\bar{1}0>$ on RXA Zircaloy-4 after 600 keV Zr^+ ions irradiation at 623 K and a dose of 0.45 dpa.

pure edge orientation, but are distributed between the first order prismatic planes $\{10\bar{1}0\}$ and the second order prismatic planes $\{11\bar{2}0\}$.

3.2.3. *Loop nature after ion irradiation*

The loop nature determination is based on the inside/outside contrast method proposed by Maher and Heyre [26] and Föll and Wilkens [27]. The loop contrast depends on its nature, the angle made by the diffraction vector with respect to the habit plane normal $\boldsymbol{n}$, but also on the sign of the Bragg deviation parameter s_g. For pure edge loops, the Burgers vectors is parallel to the habit plane normal $\boldsymbol{n}$. But, as described earlier, the <a>-loops in zirconium are non-edge loops. For this specific case, the analysis method is slightly more complicated [2,3] and Maher and Eyre [26] proposed a "safe/unsafe" method which insures to be in good conditions for the loop nature analysis. To conduct this analysis a zone axis $B \approx 11\bar{2}3$ and a diffraction vector $\mathbf{g}$ of the type $\mathbf{g} = 11\bar{2}2$ have systematically been used. Since the loop habit plane is never tilted more than 30° away from the pure edge orientation, in these diffraction conditions, two third of the loops are in a safe orientation.

It should be pointed out that, depending on the TEM, there can be an additional 180° rotation between image and diffraction pattern. The method to check the existence of this rotation is well explained by Loretto and Smallman [28]. This is critical for loop nature determination.

Fig. 9 illustrates this analysis, taking the Bragg deviation parameter s_g as positive. The loop Burgers vectors have been determined as described earlier. Following the methods described by Jostsons et al. [3], it can be seen that the loops with a Burgers vector $\frac{1}{3}[\bar{1}2\bar{1}0]$ such as loops A, B, E, F, G, H, I, M are in safe orientation. On the other hand, loops with a Burgers vector of $\frac{1}{3}[\bar{2}110]$ or $\frac{1}{3}[\bar{1}\bar{1}20]$ can be in safe or unsafe orientation. The loops in unsafe orientation can be distinguished by comparing the loop trace orientation to the orientation of the diffraction vector $\mathbf{g}$. If the loop trace is inclined by less than 30° to $\mathbf{g}$, the loop is in unsafe orientation, while if the trace is inclined by more than 30° to $\mathbf{g}$, the loop is in safe orientation. Therefore, loops C,J and L ($\mathbf{b} = \frac{1}{3}[\bar{2}110]$) are in safe orientation, while loops D and K ($\mathbf{b} = \frac{1}{3}[\bar{2}110]$) are in unsafe orientation. Indeed, the trace of this loop is reported on the stereographic projection (Fig. 9) which shows that the loop habit plane is between the first prismatic plane $(10\bar{1}0)$ (in green on the stereographic projection) and the second prismatic plane $(\bar{2}110)$ (in

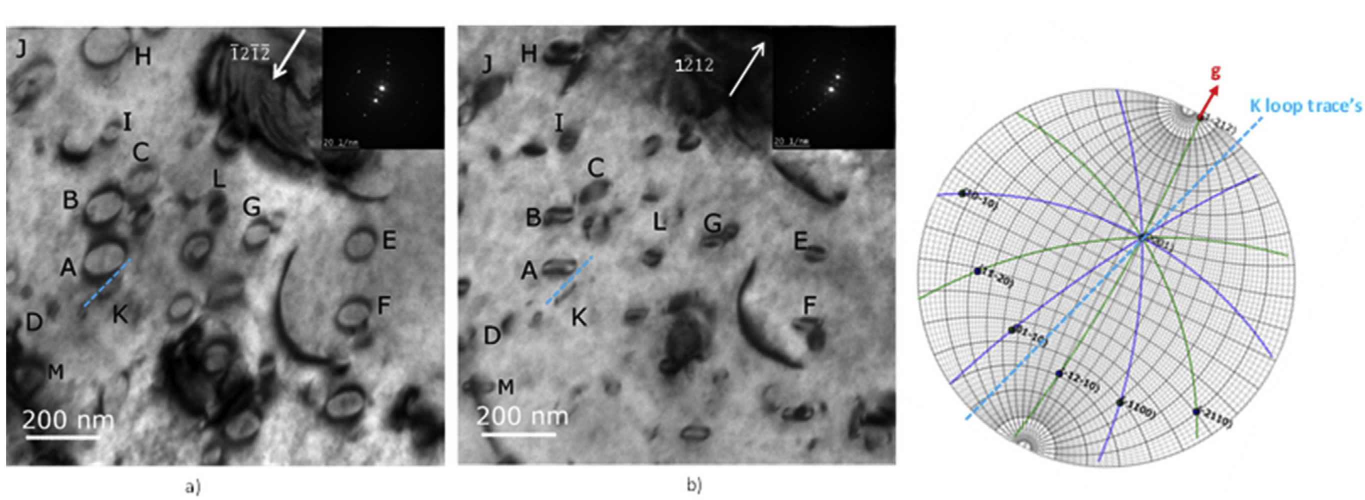

Fig. 9. Characterization of the dislocation loops nature applying the inside/outside contrast method on a Zr^+ 600 keV irradiated grain on pre-strained RXA Ziracloy-4 at 723 K and 0.45 dpa a) Outside contrast with $\mathbf{g} = \bar{1}2\bar{1}\bar{2}$ b) Inside contrast with $\mathbf{g} = 1\bar{2}12$. N~$[\bar{1}2\bar{1}3]$ λ = 26°. The stereographic projection is given for the observation tilt angle.

blue), and that the trace is inclined of less than 30° from **g**.

The loop nature analysis has been performed, after 600 keV Zr ions irradiation at 723 K, for 28 loops after a damage dose of 0.45 dpa and for 45 loops after a damage dose of 1.36 dpa. As observed in Fig. 9, all the loops analyzed show an outside contrast when **g** = $\bar{1}2\bar{1}\bar{2}$ and appear in inside contrast when **g** = $1\bar{2}12$. The loops are therefore all interstitial in nature after Zr ion irradiation at 723 K. It should be pointed out that the change of contrast is clear allowing an accurate loop nature determination. After irradiation at 673 K, because of the too small loop size, the determination of the loop nature cannot be done with confidence.

3.2.4. *Nature of the loops after electron irradiations*

The same method has been used for the characterization of loops obtained after electron irradiation at 723 K and 673 K. The analysis of the electron irradiated Zircaloy-4 at 723 K is shown on Fig. 10. For the same diffraction conditions, loops A′ and B′ show opposite contrast, proving that loop A′ is interstitial in nature and loop B′ is of vacancy nature. Among 69 loops analyzed, 65 loops were found to be interstitial in nature, while only 4 were found to be vacancy in nature. This study proves that under electron irradiation at 723 K both interstitial and vacancy loops can be present in Zircaloy-4.

This analysis has also been conducted for samples irradiated with 1 MeV electrons at 673 K (Fig. 11). For some loops, such as loops A, B, C and D, the change of contrast is clear. The loops have an inside contrast for **g** = $\bar{1}\bar{1}22$ and an outside contrast for **g** = $11\bar{2}2$, proving that they are vacancy loops. However some loops, such as E, F and G have a strong contrast for **g** = $11\bar{2}2$ but disappear with **g** = $\bar{1}\bar{1}22$. This asymmetric contrast was also noticed by Griffiths and al. [12,29] and has been explained by an adverse effect of the oxide layer on the diffraction contrast. It is therefore difficult to conclude on the nature of these specific loops. Only 18 loops have been analyzed with confidence and were all vacancies. However, interstitial loops may also be present, since the nature of several loops was not determined due to the asymmetric contrast.

An additional 1 MeV electron irradiation has been performed at 853 K on a recrystallized Ziracloy-4 sample taken in the same rolled sheet, using a higher electron flux of 8.4 × 10^{23} $e^{-}.m^{-2}$. s^{-1}. The loop nature analysis has been done, using the same method (grain with a foil normal N~[$0\bar{1}1\bar{5}$] corresponding to an angle of λ = 10°). 16 loops were analyzed and were all found to be interstitial loops. Again, several loops could not be analyzed with confidence, the loops being too small or the contrast disappearing when using the opposite diffraction vector.

3.3. *Dislocation helical climb*

In addition to the nucleation and growth of dislocation loops, the formation and growth of helix due to helical climb on linear <a>-dislocations has been observed in situ under electron irradiation at 673 K and at 723 K as illustrated on Fig. 12, showing the kinetics of helical climb under irradiation at 723 K in RXA Zircaloy-4. The evolution of the helices, mean pitch and mean amplitude has been analyzed for one dislocation at 723 K (Fig. 13). It can be observed that an increase of the amplitude of helix turns is

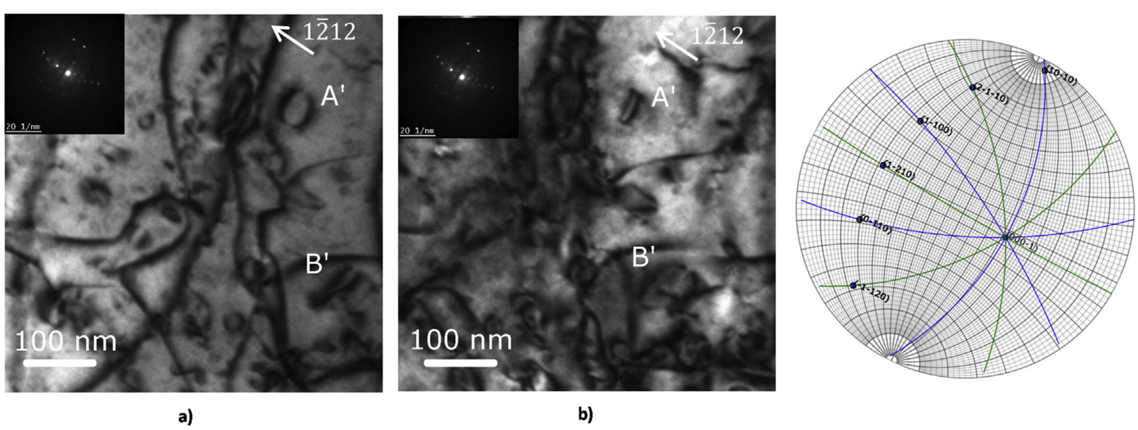

Fig. 10. Characterization of the dislocation loops nature on a 1 MeV electron irradiated grain on pre-strained RXA Zircaloy-4 at 723 K and 0,03 dpa a) g = $11\bar{2}0$ s > 0 b) g = $11\bar{2}0$ s < 0. Foil normal N~ [$1\bar{2}1\bar{6}$] λ = 14.5°. The stereographic projection is given for the observation tilt angle.

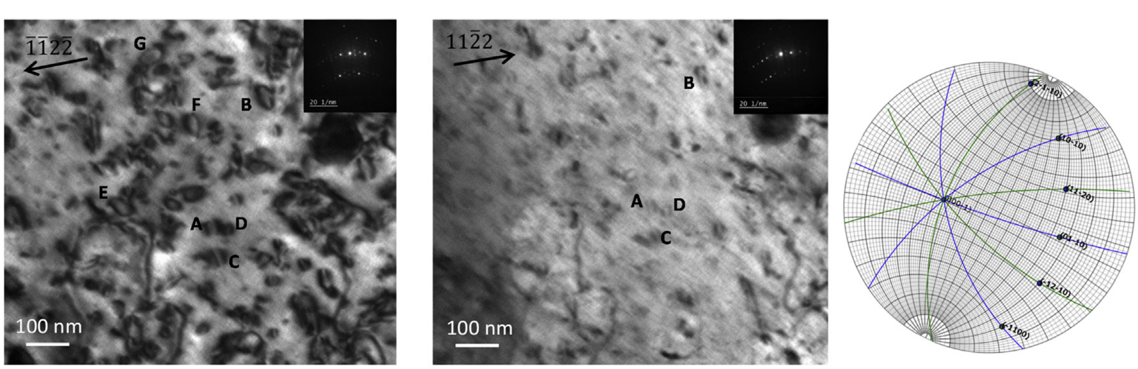

Fig. 11. Characterization of the dislocation loops nature applying the inside/outside contrast method on a 1 MeV electron irradiated grain at 673 K and 0.04 dpa on pre-strained RXA Zircaloy-4. Foil normal N~[$01\bar{1}\bar{2}$] , λ = 30°. The stereographic projection is given for the observation tilt angle.

observed while the pitch decreases. The helix pitch and amplitude seem to reach a plateau quickly after the beginning of the irradiation. Indeed, the amplitude of the helices tends to saturate around 0.04 dpa and the helix pitch saturates around 0.03 dpa.

After ion irradiation at 723 K (Fig. 14), wavy dislocations are observed. Since no glide trace on the surface are noticed, the wavy shape of the dislocation is explained by their helical climb under irradiation.

4. Discussion

4.1. Discussion on kinetics of <a>-loops evolution under 1 MeV electron irradiation

It has been shown that the loop number density increases with dose. No clear saturation of the loop number density is observed for this low damage dose (lower than 0,064 dpa). In previous experiments conducted with a higher electron flux [16,17] it was shown that the loop number density rapidly reached a saturation, which was not observed in this work. This study shows a significant decrease of the loop number density when the temperature is increased from 673 K to 723 K, in good agreement with these previous studies.

A significant dispersion in loop growth rate is observed between grains. No clear effect of temperature is observed for these low doses contrary to previous works, probably because the saturation of the loop number density was not yet reached. Indeed, it is usually observed that when the irradiation temperature increases the loop growth rate increases and the loop number density decreases [16,17].

The effect of flux could be evaluated when comparing our experiments to previous works. Indeed, it can be noticed that after about 1000 s and for a flux of 6×10^{21} $e^{-}.m^{-2}.\ s^{-1}$, the loop diameter is around 27 nm at 723 K in our experiment. For similar duration, Nakamichi et al. [17] and Hellio et al. [16] obtained respectively a loop diameter of 27 nm and 22 nm at 770 K for an improved Zircaloy-2 and a Zr-1760 ppm O alloy and for a flux of 4.6×10^{22} $e^{-}.m^{-2}.\ s^{-1}$. Considering these values, it appears that the effect of flux on the loop growth rate is relatively weak. The loop growth rate has been deduced from our data by considering the slope of the linear increase of the diameter after the transient regime, and plotted on the chart given by Nakamichi et al. for improved Zircaloy-2, for electron irradiation conducted at 570 K and 770 K (Fig. 15). The loop growth rate obtained from our electron irradiation conducted at 673 and 723 K appears to be close to the power law of the flux ϕ proposed by Nakamichi et al. $dD/dt \propto \phi^p$ with p close to 0.5. Nakamichi et al. have estimated a value for the vacancy migration energy by considering that the loop diameter (D in m) evolves as a function of the electron flux ϕ (in $e^{-}.m^{-2}.\ s^{-1}$) and of the vacancy mobility according to the equation (1) derived by Kiritani et al. [30].

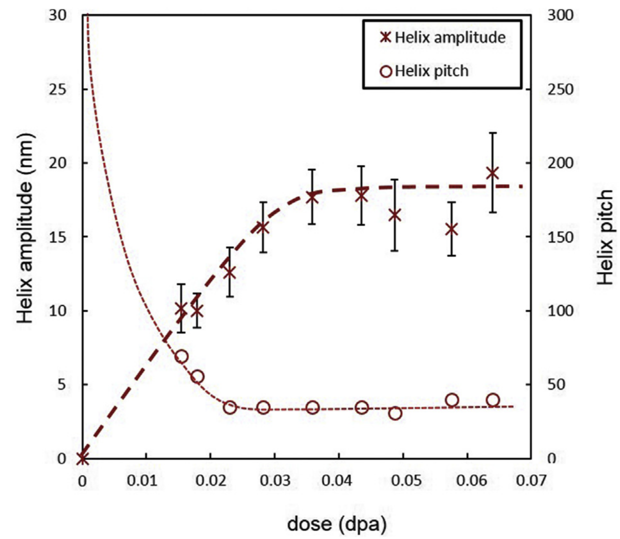

Fig. 13. Evolution of the helix amplitude and the helix pitch of the dislocation during helical climb under 1 MeV electron irradiation at 723 K on pre-strained RXA Zircaloy-4.

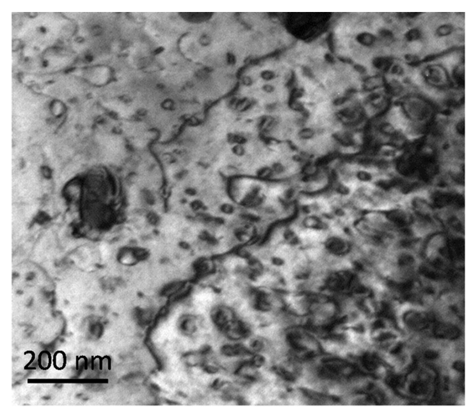

Fig. 14. Evidence of helical climb of <a>-type dislocations observed after Zr 600 keV ion irradiation at 723 K and after 1.36 dpa.

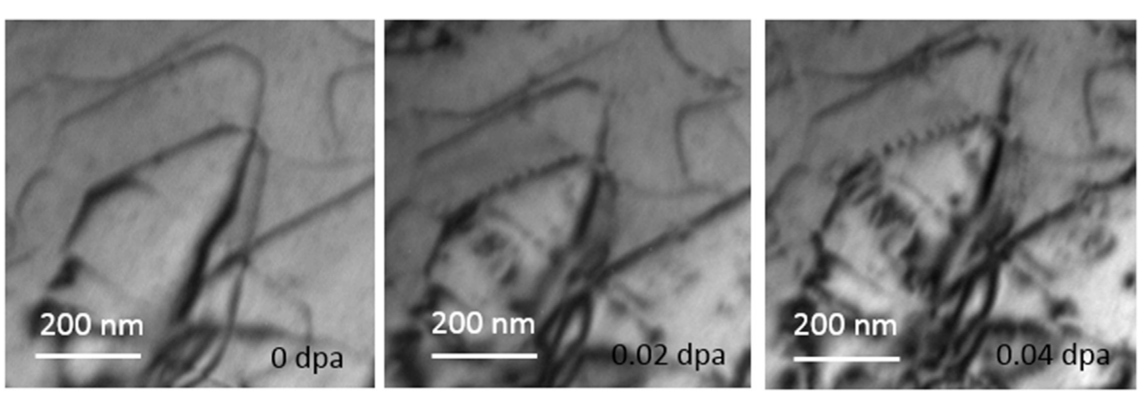

Fig. 12. Helical climb of <a>-type dislocations observed under 1 MeV electron irradiations at 723 K.

$$\frac{dD}{dt} = A_0 \cdot \phi^{\frac{1}{2}} \cdot \exp\left(-\frac{E_m^v}{2kT}\right) \tag{1}$$

According to these authors the vacancy migration energy (E_m^v) is found to be close to 1 eV. A mean square adjustment of the two parameters A_0 and E_m^v of equation (1) has been done on the values given by Nakamichi et al. in addition to our results. A value of 0.71 eV for the vacancy migration energy has been obtained which is in good agreement with the values obtained by Samolyuk et al. [31] using ab-initio simulations. The parameter A_0 is found to be equal to 2.1×10^{-20} m^2 s$^{-1/2}$.

Following the analysis proposed by Nakamichi et al. [17], the evolution of the diameter of individual loops has been plotted as a function of irradiation time in a log-log plot (Fig. 16). Nakamichi et al. show that the loop diameter evolution appears to follow a power relationship: $D \propto t^n$. The coefficient n seems to increase with temperature. Extracted from the measurement of 76 loops in two grains at 673 K and 15 loops in one grain at 723 K, the average values of coefficient n are respectively of 0.5 ± 0.3 at 673 K and 1.1 ± 0.5 at 723 K. These results shows that the evolution of the dislocation loops is almost linear with irradiation time at 723 K. This is agreement with the loop growth kinetics theory described by Kiritani [30].

4.2. Discussion on loop nature under electron irradiation

This study proves for the first time that in recrystallized Zircaloy-4 irradiated with 1 MeV electron at temperatures ranging from 673 K to 723 K (and low electron flux) vacancy loops coexist with interstitial loops. It is also shown that as the temperature increases, the proportion of interstitial loops increases. For a higher irradiation temperature (T = 853 K, and higher electron flux) only interstitial loops have been clearly observed. This last result is in agreement with Nakamichi et al. [17] and Hellio et al. [16] who found only interstitial loops at temperatures higher than 773 K. Concerning pure zirconium there is a remaining disagreement in the literature since Carpenter and Watters [11] showed that at 725 K <a>-loops were all interstitial in nature whereas Griffiths et al. [14] proved that from 675 K up to 730 K both vacancy and interstitial <a>-loops are observed, which is consistent with our results.

The fact that vacancy loops are able to nucleate and grow in zirconium alloys under electron irradiation had remained, since the early work done by Griffiths et al. [12,14] a puzzling phenomenon. Indeed, due to the preferential absorption of interstitials by dislocation loops, because of the difference in elastic interaction of vacancy and Self Interstitial Atoms (SIA) with the edge dislocation stress field, vacancy loops were assumed to shrink under irradiation and only interstitial loops were believed to be able to grow. Furthermore, in the absence of collision cascade under electron irradiation, vacancy loops were believed not to be able to nucleate. Many reasons [1,7] have been proposed to explain the nucleation and growth of both vacancy and interstitial loops under electron irradiation in zirconium and zirconium alloys, but for the time being, none has been able to meet a general agreement.

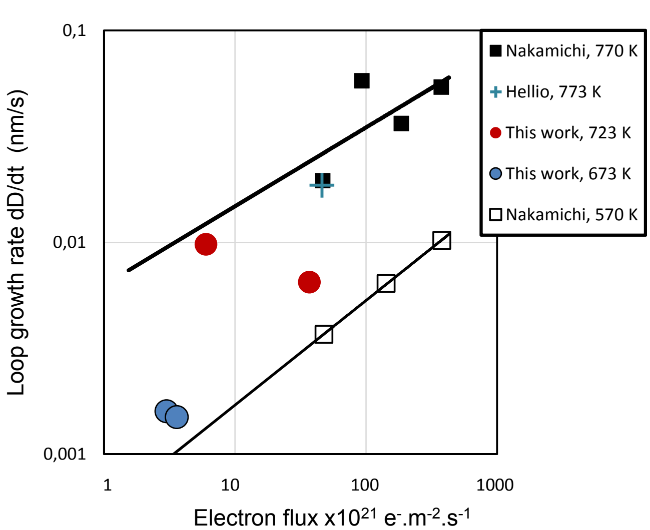

Fig. 15. Loop growth rate as a function of electron flux in zirconium alloys [16,17].

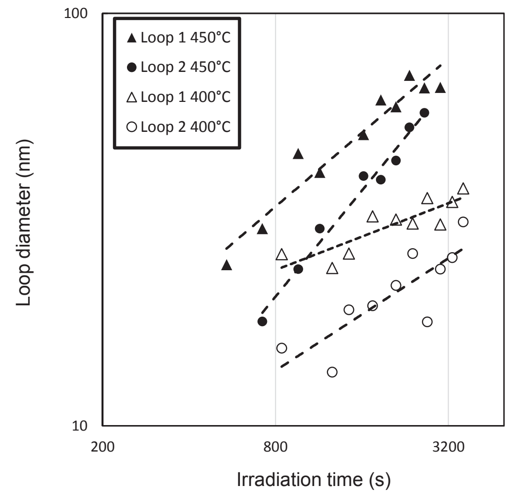

Fig. 16. Evolution of the diameter of individual loops under 1 MeV electron irradiations at 673 and 723 K for an electron flux ranged from 3×10^{21} and 6×10^{21} e$^-$.m^{-2}.s^{-1}.

The fact that at temperatures higher or equal than 770 K, mainly interstitial loops can be found in Zircaloys could be explained by the thermal emission of vacancies from vacancy loops which becomes higher than the net absorption of vacancies (vacancy absorption rate − SIA absorption rate) at high temperature. At the same time, interstitial loops continue to grow thanks to the net absorption of interstitials which remains positive.

Although the origin of the presence of vacancy loops is not understood, there is an important consequence that results from this observation. Indeed, to explain the stress free growth phenomenon, a theory based on the difference in diffusion anisotropy of interstitials and vacancy has been proposed [32]. Based on this Diffusional Anisotropy Difference (DAD), a cluster dynamics model has been developed [33]. Assuming an isotropic diffusion for vacancies, a rapid diffusion of interstitials in the basal plane and a lower diffusion along the <c>-axis, the authors have been able to compute the density of interstitial and vacancy loops as a function of the angle between the <c>-axis of the grain and the thin foil normal (λ) under 1 MeV electron irradiation. In their model, if the angle λ is below 60°, only interstitial loops are present in the thin foil. Based on our study results, and Griffiths results, where vacancy loops are observed for low λ, one can conclude that the assumed difference in anisotropic diffusion of interstitials and vacancies is in fact very weak. This is in agreement with recent ab initio and Monte-Carlo computations [31] which have shown a nearly isotropic diffusion of SIAs.

4.3. Discussion on kinetics of <a>-loops evolution under 600 keV Zr ion irradiation

The loops obtained after ion irradiation have been compared to the loops obtained after electron irradiation under similar irradiation conditions in terms of damage rate (1×10^{-4} dpa. s^{-1}), dose (0.37 dpa under electron and 0.45 dpa under ion irradiation) and temperature (723 K), and for similar grain orientation (λ between 15 and 30°). The loop number density and mean diameter observed after 600 keV Zr^{+} ion irradiation are reported along with the loop evolution under electron irradiation (Fig. 17). It is shown that for a similar dose, the loop number density is higher after ion irradiation with a value of 6.4×10^{20} m^{-3} at 0.45 dpa, while the loop number density is around 4×10^{20} m^{-3} at 0.37 dpa for electron irradiation. On the contrary, the mean loop diameter is lower under ion irradiation than under electron irradiation, with values respectively of 32 nm and 45 nm.

This result shows that under ion irradiation the nucleation of loops is favored at the expense of growth. This is due to the nature of the primary damage. Indeed, under 600 keV Zr ion irradiation large displacement cascades are formed where point defects recombination occurs, leaving only few remaining point defects free to migrate compared to electron irradiation. Within the cascades, small point defect clusters are also formed [34]. These small point defect clusters act as nuclei for the growth of <a>-loops, therefore explaining the higher loop density and lower growth rate observed under ion irradiation.

4.4. Discussion on <a>-loop nature under 600 keV Zr ion irradiation

It has been shown that after Zr ion irradiations conducted at 723 K all the analyzed loops were interstitial loops. This is surprising when considering the results obtained under electron irradiation. The main differences between these two experiments are the higher damage rate under Zr ion irradiation compared to the samples analyzed after electron irradiation and the formation of displacement cascades under Zr ion irradiation. Moreover it has been shown under electron irradiation that the proportion of interstitial loops increases with the irradiation temperature due to the emission of vacancies by vacancy loops. The same phenomenon probably also occurs under ion irradiation, but the temperature at which vacancy loops are annealed out may be lower under ion irradiation. This could then explain why only interstitial loops are observed at this temperature. However, the loops were too small at 673 K to allow the determination of their nature to confirm this hypothesis.

It is also possible that injected self-interstitial atoms can also play a role on the loop nucleation and growth (Fig. 1) by favoring the growth of interstitials loops at the expense of vacancy loops. It should also be kept in mind that in these experiments there is only one free surface during Zr ion irradiation whereas there are two free surfaces during electron irradiation.

4.5. Discussion on <a>-dislocation helical climb

Although dislocation climb is believed to be involved in the microscopic mechanisms of irradiation creep, no experimental study of the dislocation evolution under irradiation is known. This paper presents evidences of helical climb of <a> dislocations under

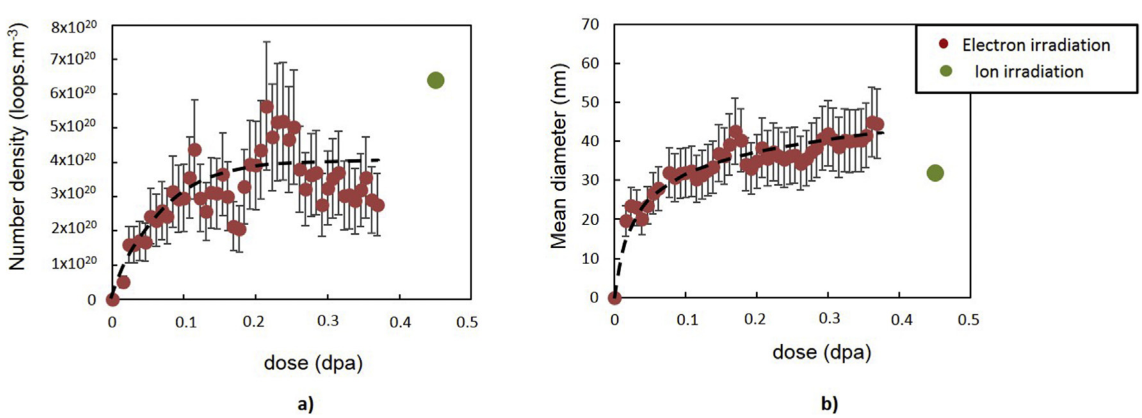

Fig. 17. Comparison between ion and electron irradiations on pre-strained RXA Zircaloy-4 at 723 K and for a damage rate of 1×10^{-4} dpa. s^{-1} a) Number density of the loops, b) Mean diameter of the loops.

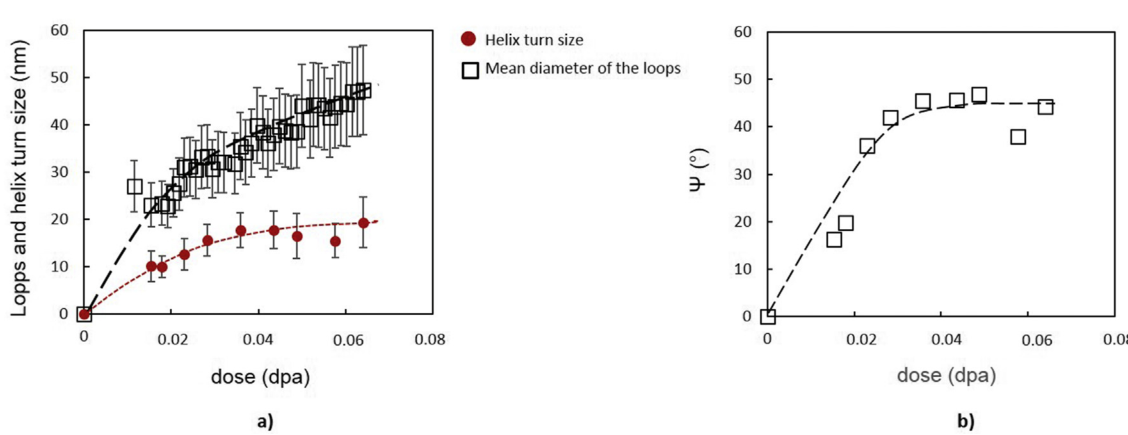

Fig. 18. 1 Mev electron irradiation at 673 K on pre-strained RXA Zircaloy-4 a) Comparison of the helix turn kinetics and loops kinetic under, b) evolution of the angle Ψ with dose.

1 MeV electron irradiation at 723 K. Several authors have also observed helical climb under electron irradiation but no detailed analysis of the dislocation kinetics was performed [10,12].

The evolution of the helix pitch (Λ) and amplitude (D) has been analyzed and shows an increase of the amplitude, and also a decrease of the pitch with irradiation dose. Moreover, at 723 K the value of the pitch Λ seems to reach a plateau for low doses (<0.04 dpa). This helix turn kinetics shows that the dislocation climb rate increases at the beginning of irradiation and then tends to saturate.

Comparison of the helix turns kinetics and loops kinetics has been performed for one grain irradiated at 723 K during 1 MeV electron irradiation (Fig. 18a)). The mean diameter of the loops observed in the same grain as the dislocations is plotted. The amplitude of the helix turns evolves with the same trend as the loop diameter. At 723 K, the helix turns amplitude tends to saturate for a dose of 0.4 dpa while the size of the loops continues to increase.

Furthermore, the helix geometry evolution has been analyzed. The angle Ψ between the dislocation line and the Burgers vector direction has been computed from the measurement of the pitch (Λ) and the amplitude (D) according to the following equation: $\tan(\Psi) = D/(\Lambda/2)$. It can be seen on (Fig. 18b)) that the angle Ψ increases at the beginning of the irradiation and the helix reaches an equilibrium "shape" with an angle Ψ between 45° and 50°. This can be explained by the fact that the shape of the helical dislocation is free to adjust itself by glide on its cylinder. According to Friedel [35] and Grilhé [36], the repulsive interaction between dislocation helical arms leads to an equilibrium angle Ψ of $\pi/4$, in good agreement with our results.

5. Conclusion

This paper presents an investigation of the microstructure evolution of recrystallized Zircaloy-4, after 1 MeV electron and 600 keV Zr^+ ion irradiations performed at 673 K and 723 K. The main findings of this experimental study are summarized below:

- The evolution of <a>-loops has been monitored during 1 MeV *in-situ* electron irradiation and ion irradiation at 673 K and 723 K. The loop number density and the mean diameter are found to increase during irradiation. An effect of the temperature has been observed on the loop number density which decreases when the irradiation temperature increases and on the loop mean diameter which increases with the temperature. Moreover, under electron irradiation, an effect of the irradiation flux has also been observed. A higher irradiation flux leads to an increase of the loop number density and a decrease of the mean diameter.
- A TEM analysis of the nature of the <a>-type loops has been performed after electron and ion irradiation. After electron irradiation, the microstructure consists of both, vacancy and interstitial loops. At 673 K, only vacancy loops were analyzed with confidence. At 723 K, both vacancy and interstitial loops have been observed with a higher proportion of interstitial loops. Under ion irradiations, on the other hand, the nature analysis of the loops has been performed for irradiation temperature of 723 K and only interstitial loops have been observed. Hypotheses have been proposed, mainly based on the point defects migration to explain such microstructures.
- Evidences of helical dislocation climb are given in this paper under electron and ion irradiations. This study brings the first experimental quantitative results on the climb mechanism.

This experimental study provides a better insight on the microstructure evolution of Zr alloys under irradiation which should lead, in a future prospect, to a better understanding and prediction of the evolution of the mechanical properties with irradiation and also of the in-reactor deformation of components made of Zr alloys.

Acknowledgments

This research work is supported by EDF and AREVA NP. We are thankful to Thierry Vandenberghe (CEA Saclay) and Sandrine Picard (CSNSM Orsay) for their help to perform the electron and ion irradiations on the different facilities, and to Thomas Jourdan (CEA Saclay) for fruitful discussion.

References

[1] F. Onimus, J.L. Béchade, Radiation effects in zirconium alloys, in: Comprehensive Nuclear Materials, Elsevier, 2012, pp. 1–31.
[2] P.M. Kelly, R.G. Blake, The characterization of dislocation loops in neutron irradiated zirconium, Philos. Mag. 28 (2) (Aug. 1973) 415–426.
[3] A. Jostsons, P.M. Kelly, R.G. Blake, The nature of dislocation loops in neutron irradiated zirconium, J. Nucl. Mat. 66 (3) (May 1977) 236–256.
[4] A. Jostsons, P. Kelly, R. Blake, K. Farrell, Neutron irradiation-induced defect structures in zirconium, in: J. Sprague, D. Kramer (Eds.), Effects of Radiation on Structural Materials, ASTM International, 100 Barr Harbor Drive, PO Box C700, West Conshohocken, PA 19428-2959, 1979, 46–46–16.
[5] R.W. Gilbert, K. Farrell, C.E. Coleman, Damage structure in zirconium alloys neutron irradiated at 573 to 923 k, J. Nucl. Mat. 84 (1–2) (Oct. 1979) 137–148.
[6] D.O. Northwood, et al., Characterization of neutron irradiation damage in zirconium alloys — an international 'round-robin' experiment, J. Nucl. Mat. 79 (2) (Feb. 1979) 379–394.
[7] M. Griffiths, A review of microstructure evolution in zirconium alloys during irradiation, J. Nucl. Mat. 159 (Oct. 1988) 190–218.
[8] G.J.C. Carpenter, D.O. Northwood, The contribution of dislocation loops to radiation growth and creep of Zircaloy - 2, J. Nucl. Mat. 56 (3) (Jun. 1975) 260–266.
[9] G.S. Was, Fundamentals of Radiation Materials Science: Metals and Alloys, second ed., Springer, New York, 2017.
[10] S.N. Buckley, S.A. Manthorpe, Dislocation loop nucleation and growth in zirconium-2.5 wt% niobium alloy during 1 MeV electron irradiation, J. Nucl. Mat. 90 (1–3) (May 1980) 169–174.
[11] G.J.C. Carpenter, J.F. Watters, A study of electron irradiation damage in Zirconium using a high voltage electron microscope, J. Nucl. Mat. 96 (3) (Feb. 1981) 213–226.
[12] M. Griffiths, M.H. Loretto, R.E. Smallman, Electron damage in zirconium I, J. Nucl. Mat. 115 (2–3) (Apr. 1983) 313–322.
[13] M. Griffiths, M.H. Loretto, R.E. Smallman, Electron damage in zirconium II, J. Nucl. Mat. 115 (2–3) (Apr. 1983) 323–330.
[14] M. Griffiths, M.H. Loretto, R.E. Smallman, Anisotropic distribution of dislocation loops in HVEM-irradiated Zr, Philos. Mag. A 49 (5) (Nov. 1984) 613–624.
[15] M. Griffiths, R.C. Styles, C.H. Woo, F. Phillipp, W. Frank, Study of point defect mobilities in zirconium during electron irradiation in a high-voltage electron microscope, J. Nucl. Mat. 208 (3) (Feb. 1994) 324–334.
[16] C. Hellio, C.H. de Novion, L. Boulanger, Influence of alloying elements on the dislocation loops created by Zr+ ion or by electron irradiation in α-zirconium, J. Nucl. Mat. 159 (Oct. 1988) 368–378.
[17] H. Nakamichi, C. Kinoshita, K. Yasuda, S. Fukada, Formation and growth process of dislocation loops in Zircaloys under electron irradiation, J. Nucl. Sci. Technol. 34 (11) (Nov. 1997) 1079–1086.
[18] D. Lee, E.F. Koch, Irradiation damage in Zircaloy-2 produced by high-dose ion bombardment, J. Nucl. Mat. 50 (2) (Mar. 1974) 162–174.
[19] R. Adamson, W. Bell, D. Lee, Use of ion bombardment to study irradiation damage in zirconium alloys, in: J. Schemel, H. Rosenbaum (Eds.), Zirconium in Nuclear Applications, ASTM International, 100 Barr Harbor Drive, PO Box C700, West Conshohocken, PA 19428-2959, 1974, pp. 215–228.
[20] R.M. Hengstler-Eger, et al., Heavy ion irradiation induced dislocation loops in AREVA's M5® alloy, J. Nucl. Mat. 423 (1–3) (Apr. 2012) 170–182.
[21] Y. Idrees, Z. Yao, M.A. Kirk, M.R. Daymond, In situ study of defect accumulation in zirconium under heavy ion irradiation, J. Nucl. Mat. 433 (1–3) (Feb. 2013) 95–107.
[22] E.E. Underwood, Stereology, or the quantitative evaluation of microstructures, J. Microsc. 89 (2) (Apr. 1969) 161–180.
[23] O.S. Oen, Cross Sections for Atomic Displacements in Solids by Fast Electrons, Oak Ridge National Laboratory, Aug-1973.
[24] M. Griffiths, Displacement energies for Zr measured in a HVEM, J. Nucl. Mat. 165 (3) (Jun. 1989) 315–317.
[25] R.E. Stoller, M.B. Toloczko, G.S. Was, A.G. Certain, S. Dwaraknath, F.A. Garner, On the use of SRIM for computing radiation damage exposure, Nucl. Instrum. Methods Phys. Res. Sect. B Beam Interact. Mat. At. 310 (Sep. 2013) 75–80.
[26] D.M. Maher, B.L. Eyre, Neutron irradiation damage in molybdenum, Philos. Mag. 23 (182) (Feb. 1971) 409–438.

[27] H. Föll, M. Wilkens, A simple method for the analysis of dislocation loops by means of the inside-outside contrast on transmission electron micrographs, Phys. Status Solidi A 31 (2) (Oct. 1975) 519–524.

[28] M.H. Loretto, R.E. Smallman, Defect Analysis in Electron Microscopy, Chapman and Hall;; Wiley: Distributed by Halstead Press, London; New York, 1975.

[29] M. Griffiths, J. White, R. E. Smallman, M. H. Loretto, and I. P. Jones, "Asymmetric ±g contrast in oxidised Zr and Ti," presented at the Proc. 10th Int. Cong. on Electron Microscopy, Hamburg, 1982, p. 105.

[30] M. Kiritani, N. Yoshida, H. Takata, Y. Maehara, Growth of interstitial type dislocation loops and vacancy mobility in electron irradiated metals, J. Phys. Soc. Jpn. 38 (6) (Jun. 1975) 1677–1686.

[31] G.D. Samolyuk, A.V. Barashev, S.I. Golubov, Y.N. Osetsky, R.E. Stoller, Analysis of the anisotropy of point defect diffusion in hcp Zr, Acta Mat. 78 (Oct. 2014) 173–180.

[32] C.H. Woo, Theory of irradiation deformation in non-cubic metals: effects of anisotropic diffusion, J. Nucl. Mat. 159 (Oct. 1988) 237–256.

[33] F. Christien, A. Barbu, Effect of self-interstitial diffusion anisotropy in electron-irradiated zirconium: a cluster dynamics modeling, J. Nucl. Mat. 346 (2–3) (Nov. 2005) 272–281.

[34] F. Gao, D.J. Bacon, A.F. Calder, P.E.J. Flewitt, T.A. Lewis, Computer simulation study of cascade overlap effects in α-iron, J. Nucl. Mat. 230 (1) (May 1996) 47–56.

[35] J. Friedel, Dislocations, Pergamon Press, Oxford; New York, 1964. U.S.A. ed. distributed by Addison-Wesley Pub. Co., Reading, Mass.

[36] J. Grilhé, Formes d'équilibre des dislocations hélicoïdales, J. Phys. Colloq. 27 (C3) (Jul. 1966). C3-183-C3-187.